JACC: CARDIOVASCULAR IMAGING VOL. ■, NO. ■, 2017
ISSN 1936-878X
http://dx.doi.org/10.1016/j.jcmg.2017.06.006

Cardiac-Specific Conversion Factors to Estimate Radiation Effective Dose From Dose-Length Product in Computed Tomography

Sigal Trattner, PhD,[a] Sandra Halliburton, PhD,[b] Carla M. Thompson, PhD,[c] Yanping Xu, PhD,[d] Anjali Chelliah, MD,[e] Sachin R. Jambawalikar, PhD,[f] Boyu Peng, MS,[g] M. Robert Peters, MD,[h] Jill E. Jacobs, MD,[i] Munir Ghesani, MD,[j] James J. Jang, MD,[k] Hussein Al-Khalidi, PhD,[l] Andrew J. Einstein, MD, PhD[m]

ABSTRACT

OBJECTIVES This study sought to determine updated conversion factors (*k*-factors) that would enable accurate estimation of radiation effective dose (ED) for coronary computed tomography angiography (CTA) and calcium scoring performed on 12 contemporary scanner models and current clinical cardiac protocols and to compare these methods to the standard chest *k*-factor of 0.014 $mSv \cdot mGy^{-1}cm^{-1}$.

BACKGROUND Accurate estimation of ED from cardiac CT scans is essential to meaningfully compare the benefits and risks of different cardiac imaging strategies and optimize test and protocol selection. Presently, ED from cardiac CT is generally estimated by multiplying a scanner-reported parameter, the dose-length product, by a *k*-factor which was determined for noncardiac chest CT, using single-slice scanners and a superseded definition of ED.

METHODS Metal-oxide-semiconductor field-effect transistor radiation detectors were positioned in organs of anthropomorphic phantoms, which were scanned using all cardiac protocols, 120 clinical protocols in total, on 12 CT scanners representing the spectrum of scanners from 5 manufacturers (GE, Hitachi, Philips, Siemens, Toshiba). Organ doses were determined for each protocol, and ED was calculated as defined in International Commission on Radiological Protection Publication 103. Effective doses and scanner-reported dose-length products were used to determine *k*-factors for each scanner model and protocol.

RESULTS *k*-Factors averaged 0.026 $mSv \cdot mGy^{-1}cm^{-1}$ (95% confidence interval: 0.0258 to 0.0266) and ranged between 0.020 and 0.035 $mSv \cdot mGy^{-1}cm^{-1}$. The standard chest *k*-factor underestimates ED by an average of 46%, ranging from 30% to 60%, depending on scanner, mode, and tube potential. Factors were higher for prospective axial versus retrospective helical scan modes, calcium scoring versus coronary CTA, and higher (100 to 120 kV) versus lower (80 kV) tube potential and varied among scanner models (range of average *k*-factors: 0.0229 to 0.0277 $mSv \cdot mGy^{-1}cm^{-1}$).

CONCLUSIONS Cardiac *k*-factors for all scanners and protocols are considerably higher than the *k*-factor currently used to estimate ED of cardiac CT studies, suggesting that radiation doses from cardiac CT have been significantly and systematically underestimated. Using cardiac-specific factors can more accurately inform the benefit-risk calculus of cardiac-imaging strategies. (J Am Coll Cardiol Img 2017;■:■–■) © 2017 The Authors. Published by Elsevier on behalf of the American College of Cardiology Foundation. This is an open access article under the CC BY-NC-ND license (http://creativecommons.org/licenses/by-nc-nd/4.0/).

From the [a]Department of Medicine, Division of Cardiology, Columbia University Medical Center, and New York-Presbyterian Hospital; [b]Imaging Institute, Division of Radiology, Cleveland Clinic, Cleveland, Ohio, and Lerner Research Institute, Department of Biomedical Engineering, Cleveland Clinic, Cleveland, Ohio, and Department of Chemical and Biomedical Engineering, Cleveland State University, Cleveland, Ohio, and Philips Healthcare, Cleveland, Ohio; [c]Imaging Institute, Division of Radiology, Cleveland Clinic, and Lerner Research Institute, Department of Biomedical Engineering, Cleveland Clinic, and Department of Chemical and Biomedical Engineering, Cleveland State University, Cleveland, Ohio; [d]Radiological Research Accelerator Facility, Center for Radiological Research, Columbia University Medical Center, Irvington, New York; [e]Department of Pediatrics, Division of Pediatric Cardiology, New York-Presbyterian Morgan Stanley Children's Hospital, and Columbia University Medical Center, New York, New York; [f]Department of Radiology, Columbia University Medical Center, and

ABBREVIATIONS AND ACRONYMS

CT = computed tomography

CTA = computed tomography angiography

DLP = dose-length product

ED = effective dose

kVp = kilovolt peak

MOSFET = metal-oxide semiconductor field-effect transistor

Cardiac computed tomography (CT) has experienced tremendous advances in the past decade. Growing evidence supports the role of coronary artery calcium scoring for risk stratification, and some guidelines now recommend it as a reasonable test for asymptomatic adults at intermediate risk (1). Coronary computed tomography angiography (CTA) has demonstrated high accuracy for diagnosing obstructive coronary artery disease (2), the ability to improve prognostication (3), and in some settings, capability to more rapidly and cost-effectively diagnose chest pain in patients (4). In many clinical contexts, coronary CTA now stands as an option that can be selected to guide optimal patient management and incorporated into clinical pathways (5,6).

Each cardiac imaging modality has strengths and weaknesses, and optimizing management requires a weighting of these features for each option in the context of the patient and clinical question. One particular concern for coronary CTA is its associated radiation burden. Although initial studies found high radiation dose and risk (7), numerous technical advances such as prospectively triggered axial scan modes, lower tube potentials, and iterative image reconstruction now enable, in the best-case scenario, performing coronary CTA with extremely low radiation burden, comparable to that of several chest radiographs (8). However, such low coronary CTA doses require a confluence of several factors: availability of these technical advances which are not all implemented on entry level scanners, operator expertise, favorable patient heart rate and rhythm and habitus, and willingness to tolerate some image noise and limitation in the number of phases of the cardiac cycle available for interpretation. Thus, although some patients will receive extremely low doses, many will still receive considerably higher doses. Indeed, contemporary coronary CTA practice is characterized by a wide range of radiation doses among laboratories and among patients (9), and thus the benefit-risk calculus of coronary CTA and its comparison with other modalities may vary depending on the particular radiation dose. In particular, when taking care of patients with chest pain, the physician's choice between coronary CTA and nuclear myocardial perfusion imaging may depend in part on radiation burden. Such comparison is predicated on accurate radiation dosimetry for both examinations.

The single parameter most commonly used to compare ionizing radiation burdens among different imaging modalities, scanners, and protocols is the effective dose (ED), in units of millisieverts (mSv). Effective dose characterizes whole-body exposure from a nonuniform radiation exposure as a weighted average of organ absorbed doses. It is presently defined in accordance with a formulation specified by the International Commission on Radiological Protection (ICRP) in its Publication 103 (10) as the sum over all specified organs of doubly weighted organ-absorbed doses, where weights reflect both the relative sensitivity of each organ to radiation and the radiation source. Effective dose is not without limitations (11,12); for example, the organ weights are averages for all ages and both sexes, thus precluding a sex-specific ED; and ED is not patient-size dependent. Accordingly, ED is not designed for patient-specific radiation risk assessment. Nevertheless it remains the only metric that can be easily used to compare whole-body radiation exposure across modalities and protocols. This has led to its great popularity in clinical publications and practice. ICRP Publication 103 (10) updated the radiation weighting factors for each organ based

New York-Presbyterian Hospital, New York, New York; [g]Department of Radiology, Columbia University Medical Center, and New York-Presbyterian Hospital, New York, New York; [h]Advanced Cardiovascular Imaging, New York, New York; [i]Section of Cardiac Imaging, Department of Radiology, New York University School of Medicine, and New York University Langone Medical Center, New York, New York; [j]Division of Nuclear Medicine, Department of Radiology, New York University, and New York University Langone Medical Center, New York, New York; [k]Division of Cardiology, Kaiser Permanente San Jose Medical Center, San Jose, California; [l]Duke Clinical Research Institute, Duke University Medical Center, Durham, North Carolina; and the [m]Department of Medicine, Cardiology Division, and Department of Radiology, Columbia University Medical Center, and New York Presbyterian Hospital, New York, New York. This study was supported by National Institutes of Health/National Heart, Lung, and Blood Institute grant R01 HL109711. Dr. Einstein is supported by Herbert Irving Associate Professorship and Victoria and Esther Aboodi Cardiology Researcher. Dr. Halliburton has received institutional research grants to Cleveland Clinic from Philips Healthcare and Siemens Healthcare; and is currently an employee of Philips Healthcare (her role in data collection and analysis was all performed as an employee of Cleveland Clinic, prior to her employment by Philips Healthcare). Dr. Peters has received institutional research grants from and served on the speakers' bureau of Toshiba America Medical Systems. Dr. Einstein has received institutional research grants from GE Healthcare, Philips Healthcare, and Toshiba America Medical Systems. All other authors have reported that they have no relationships relevant to the contents of this paper to disclose. Dr. Thompson's current affiliation is Vanderbilt University, Nashville, Tennessee. Dr. Xu's current affiliation is Department of Physics, East Carolina University, Greenville, North Carolina.

Manuscript received January 3, 2017; revised manuscript received May 26, 2017, accepted June 5, 2017.

FIGURE 1 **Anthropomorphic Phantom and Axial CT Image Sample Obtained in a Cardiac CT Scan**

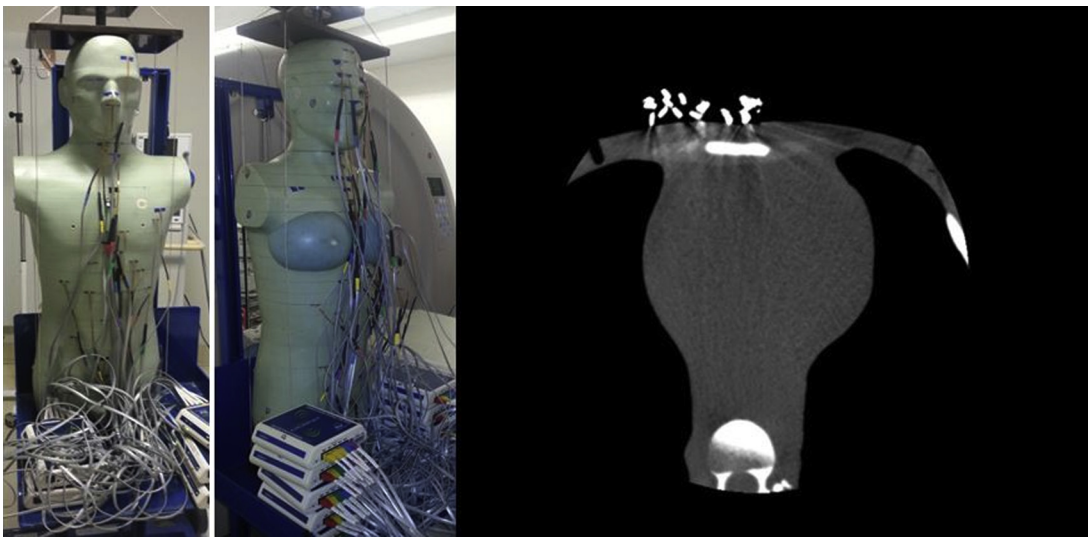

Anthropomorphic phantom assembled with MOSFETs in place and an axial image sample obtained in a cardiac CT scan of the phantom. **(Left)** Male phantom; **(middle)** female phantom; **(right)** cardiac CT image. CT = computed tomography; MOSFET = metal-oxide semiconductor field-effect transistor.

on a comprehensive, updated review of radioepidemiological and radiobiological evidence and refined methodology in comparison with the previous specification of ED in ICRP Publication 60 (13).

By far, the simplest and most commonly used method to estimate ED for CT scans is by multiplying another radiation parameter, the dose-length product (DLP), by a conversion factor, often referred to as the *k*-factor. Dose-length product, which is limited to CT, is reported on the scanner console after each CT scan and reflects both the intensity of the radiation exposure (in milligray) and the craniocaudal length irradiated (in centimeters). The *k*-factor that is conventionally used for cardiac scans, 0.014 $mSv \cdot mGy^{-1} \cdot cm^{-1}$, was introduced in European Commission guidelines for chest CT scans (14) and later adopted by the American Association of Physicists in Medicine (15). Using this chest *k*-factor to estimate ED from cardiac CT has limitations that potentially compromise the accuracy of ED estimates. First, the chest *k*-factor was never designed for cardiac studies but rather for thoracic CT; second, it is based on the older, now superseded, ICRP 60 definition of ED; and third, it was determined using three single-slice scanners, which technologically, are markedly different from the CT scanners currently in use for cardiac CT. Moreover, the European Commission guidelines document (14) had in fact provided 2 different chest *k*-factors: 0.019 $mSv \cdot mGy^{-1} \cdot cm^{-1}$ (in its Appendix A) and 0.014 $mSv \cdot mGy^{-1} \cdot cm^{-1}$ (in its Appendix C).

Thus, updated dosimetric methodology is essential to ensure accurate estimation of ED from cardiac CT. Heretofore, there has been no systematic attempt to determine *k*-factors for the diversity of scanner models and protocols used in cardiac CT practice, and the *k*-factors in published studies covering a limited combination of scanners and modes (Table 1) have not been widely adopted. In the present study, we systematically determined *k*-factors for all contemporary cardiac coronary CTA scanner designs and protocols to provide a single source of data that could be used to more accurately estimate ED of cardiac CT. Our approach was to estimate EDs from measurements performed using solid-state metal-oxide-semiconductor field-effect transistor (MOSFET) dosimeters placed in an anthropomorphic phantom and to determine *k*-factors relating these EDs to scanner-reported DLPs.

METHODS

PHANTOM. A whole-body adult anthropomorphic dosimetry verification phantom (Figure 1) was used for all experiments (ATOM 701; CIRS, Norfolk, Virginia). The phantom weighs 73 kg and has thoracic dimensions of 23 × 32 cm without breasts. It is constructed from tissue-equivalent resins and polymers that represent the body's anatomy and

radiation attenuation characteristics at diagnostic photon energies, and thus, it both physically and radiographically simulates an adult patient. The phantom is composed of a stack of 25-mm-thick contiguous transverse sections, each of which contains several 5-mm-diameter holes through which detectors can be placed for organ dose measurements. In these holes, tissue-equivalent MOSFET holders were used to place the MOSFET detectors. Holes in which MOSFETs were not placed were filled with tissue-equivalent plugs. For female scans, medium-sized tissue-equivalent breast phantoms were constructed from actual CT data of a female lying in the supine position and affixed to the body phantom. Further methodologic details for all sections are provided in the Online Appendix.

MOSFET DOSIMETERS AND ORGAN DOSE DETERMINATION. Organ dosimetry was performed using a mobile MOSFET dose verification system (TN-RD-70W, Best Medical, Ottawa, Ontario, Canada), associated with high-sensitivity MOSFETs (TN-1002RD-H, Best Medical). Voltage (in millivolt [mV]) readings were translated to dose (mGy) by calibration of the MOSFETs, using an ion chamber (10X6-3CT, Radcal, Monrovia, California) with a control unit (Accu-Dose 2186, Radcal), and a standard 32-cm-diameter cylinder poly (methyl methacrylate) phantom (West Physics Consulting, Atlanta, Georgia), according to the calibration scheme of Trattner et al. (16). Separate calibration factors were determined for each x-ray tube potential used for cardiac scan modes due to MOSFET sensitivity to energy spectra.

MOSFETs were positioned within the phantom in all 27 internal organs contributing to ED determination (10). The MOSFET voltage reading X_{tissue} in a given tissue was translated to dose D_{tissue} in that tissue by

$$D_{tissue} = f_{tissue} \cdot CF \cdot X_{tissue,}$$

where the calibration factor, CF, is in units of mGy/mV, and f_{tissue} is a scaling factor which converts dose-in-air to dose-in-tissue at the effective energy E_{eff} of x-rays used and is defined as:

$$f_{tissue}(E_{eff}) = 1 \cdot \frac{(\mu_{en}/\rho)_{tissue}}{(\mu_{en}/\rho)_{air}},$$

that is, the ratio of the mass energy-absorption coefficient μ_{en}/ρ of the specific tissue to that of air (15). Mass energy absorption coefficients were obtained from data tabulated by the National Institute of Standards and Technology at the appropriate effective energy (17), which was determined based on information obtained from the CT manufacturers (17) or, if not available, simulations using the Monte Carlo radiation transport program MCNP/MCNPX (Los Alamos National Laboratory, Los Alamos, New Mexico) to obtain effective energies. These simulations were validated with known values of effective energy.

To characterize doses to the 27 organs, we used 44 and 41 MOSFETs for female and male phantoms, respectively. Doses in larger or highly radiosensitive organs such as lungs and female breasts were determined based on measurements in multiple MOSFETs (Table 2), and an average was used to estimate the organ-absorbed dose. For lung, a weighted average was taken in which the weight for each MOSFET reading was determined by the percentage of the lung's volume surrounding the relevant MOSFET. Bone surface and bone marrow doses were measured in 8 different MOSFET locations, and a weighted average was determined according to their mass as specified by Eckerman et al. (18).

CT SCANNERS. Twelve contemporary CT scanner models representing all 5 major CT manufacturers were studied. These scanner models were chosen based on their use in the PROMISE (PROspective Multicenter Imaging Study for Evaluation of Chest Pain) trial, a 193-site, pragmatic comparative effectiveness trial which randomized outpatients with chest pain to initial testing with either coronary CTA or functional testing (5), performed in local laboratories. Therefore, the CT scanner models used reflect those used in current clinical practice. All models have either single or dual x-ray sources, and between 32 and 320 detector rows available for cardiac imaging. We performed medical physics experiments in physical anthropomorphic phantoms using one scanner of each model. Experiments were performed on multiple scanners at New York-Presbyterian Hospital/Columbia University Medical Center and at the Cleveland Clinic, Cleveland, Ohio, and on single scanners at several additional facilities (Table 3).

PROTOCOLS SCANNED. A variety of protocols are used for cardiac imaging in contemporary scanners, with the particular protocol options differing among scanners. Components of a protocol include the scan mode, tube potential, and other scan parameters. Almost all scanners have a retrospectively gated low-pitch helical mode, generally with an option for echocardiogram (ECG)-controlled tube current modulation which lowers the x-ray tube current to ≤20% of its maximum, except during a designated portion of the cardiac cycle. Most newer and all higher-end scanners have in addition at least one prospectively triggered scan mode which turns the x-ray beam off except during a designated portion of the

TABLE 1 Cardiac *k*-Factors in Published Studies

Scanner	Cardiac Protocol	Scan Length (cm)	*k*-factor ICRP 103 (mSv·mGy^{-1}cm^{-1})	*k*-factor ICRP 60 (mSv·mGy^{-1}cm^{-1})	Methodology	First Author (Ref. #)
GE LightSpeed VCT	Retrospectively ECG-gated helical 80, 100, 120, 140 kVp	16	0.0204–0.0268	NS	Monte Carlo dosimetry*	Huda et al. (22)
GE LightSpeed VCT, GE HD750	Prospectively ECG-triggered axial 100, 120, 140 kVp	NS	Median 0.028	NS	Monte Carlo dosimetry*	Gosling et al. (25,26)
Siemens SOMATOM Sensation 64	Retrospectively ECG-gated helical 80, 100, 120, 140 kVp	16	0.0264–0.0274	NS	Monte Carlo dosimetry*	Huda et al. (22)
Siemens SOMATOM Definition AS+	Retrospectively ECG-gated helical, Prospectively ECG-triggered axial 100, 120 kVp	15	0.032	0.024	Physical dosimetry	Fink et al. (27)
Siemens SOMATOM Definition AS+	Retrospectively ECG-gated helical 80, 100, 120, 140 kVp	16	0.0217–0.0282	NS	Monte Carlo dosimetry*	Huda et al. (22)
Siemens SOMATOM Definition AS+	Retrospective ECG-gated helical 100, 120, 140 kVp	12.5	0.031–0.032	NS	Monte Carlo dosimetry†	Christner et al. (28)
Siemens SOMATOM Definition	Retrospectively ECG-gated helical, Prospectively ECG-triggered axial 100, 120 kVp	15	0.028	0.021	Physical dosimetry	Fink et al. (27)
Siemens SOMATOM Definition Flash	Retrospectively ECG-gated helical, Prospectively ECG-triggered axial, Prospectively ECG-triggered helical 100, 120 kVp	13.5, 15	0.034	0.028	Physical dosimetry	Goetti et al. (29)
Siemens SOMATOM Definition Flash	Retrospectively ECG-gated helical, Prospectively ECG-triggered axial, Prospectively ECG-triggered helical 100, 120 kVp	15, 16.8	0.023	0.018	Physical dosimetry	Fink et al. (27)
Toshiba Aquilion 64	Retrospectively ECG-gated helical 120 kVp	NS	0.019–0.043 Mean 0.030	0.017–0.030 Mean 0.024	Monte Carlo dosimetry‡	Geleijns et al. (21)
Toshiba Aquilion 64	Retrospectively ECG-gated helical 120 kVp	NS	0.026	0.020	Monte Carlo dosimetry§	Geleijns et al. (21)
Toshiba Aquilion ONE	Retrospectively ECG-gated helical, Prospectively ECG-triggered helical, Prospectively ECG-triggered volume 100, 120 kVp	14	0.027–0.034	0.020–0.024	Physical dosimetry	Einstein et al. (19)
Toshiba Aquilion ONE	Retrospectively ECG-gated helical, Prospectively ECG-triggered volume 120 kVp	14	(Retro) 0.025 (Pro) 0.022	(Retro) 0.020 (Pro) 0.017	Physical dosimetry	Seguchi et al. (30)

Cardiac *k*-factors for adults reported in the literature by different groups, calculated using either physical dosimetry (various phantoms and dosimeters) or using a computational approach (simulations). These *k*-factors were for different scanners, scan modes, and parameters as tabulated. *ImPACT = CT patient dosimetry calculator (version 1.0, ImPACT 2009), using NRPB Monte Carlo dose data. †ImPACT = CT patient dosimetry calculator (version 0.9x, ImPACT 2006) using NRPB Monte Carlo dose data. ‡Algorithm based on the Electron Gamma Shower V4 (EGS4) code in combination with low-energy photon-scattering expansion that was developed by the National Laboratory for High Energy Physics (Japan). §ImPACT version number was not reported.

CT = computed tomography; ECG = electrocardiography; NRPB = National Radiological Protection Board; Pro = prospectively ECG-triggered volume, 120 kVp; Retro = retrospectively ECG-gated helical, 120 kVp.

cardiac cycle, most commonly diastasis. Additional "padding" of x-ray exposure time may be performed enabling reconstruction of additional phases of the cardiac cycle. Prospectively ECG-triggered scanning is most commonly axial but may be helical, sometimes with a high pitch, or a volume scan with no movement of the patient couch.

Typical protocols for each cardiac mode were determined for each scanner studied based on discussion with physicists and applications specialists from the vendor, as well as experienced radiologists, cardiologists, and technologists at each collaborating site. Since *k*-factors may vary based on photon energy (19), scans were generally performed for each scanner and scan mode at tube potentials of 80, 100, and 120 kVp, unless a tube potential was not available on the scanner or the scan mode was not typically used at a particular tube potential. In addition, for a few scanners, scans for determining *k*-factors were performed using less commonly used tube potentials of 70, 135, and 140 kVp. In some cases, to optimize MOSFET statistics, scans were performed at a tube current higher than that which would be used in clinical practice. The choice of tube current does not affect *k*-factors because both DLP and MOSFET voltages scale linearly with tube current. In all other respects, scans were performed with parameters mimicking those typically used clinically for that protocol. In addition to coronary CTA protocols, coronary artery calcium scoring scans were performed for most scanners. A simulator was used to generate the ECG signal ("chicken heart") for all studies. Most scans were performed using a signal simulating normal sinus rhythm at 60 beats/min; in a few cases, where a protocol is

TABLE 2 Organs and Assigned MOSFETs for Organ Dosimetry in the Phantom

Organ*	Number of MOSFETs	Weighting Factor ICRP Publication 103	Weighting factor ICRP Publication 60
Brain	6	0.01	In remainder
Salivary gland	1	0.01	–
Red bone marrow	5	0.12	0.12
Bone surface	5	0.01	0.01
Thyroid	1	0.04	0.05
Lung	5	0.12	0.12
Esophagus	3	0.04	0.05
Breast	Male:1 Female:2	0.12	0.05
Stomach	1	0.12	0.12
Liver	3	0.04	0.05
Colon	3	0.12	0.12
Bladder	1	0.04	0.05
Gonads	1	0.08	0.20
Remainder†	11	0.12	0.05

Organ list of the adult anthropomorphic phantom, with the number of MOSFETs used for dosimetry experiments and tissue (organ)-weighting factors as defined in ICRP publication 103 and ICRP publication 60. *Skin was not included. †Remainder organs in ICRP 103 definition of effective dose: adrenals, extrathoracic region, gall bladder, heart, kidneys, oral mucosa, pancreas, prostate, small intestine, spleen, thymus, uterus/cervix, without lymphatic nodes and muscle (each remainder organ had a tissue weight of 0.12/11= 0.0109). Remainder organs in ICRP 60 definition of effective dose: adrenals, brain, upper large intestine, small intestine, kidneys, muscle, pancreas, spleen, thymus, and uterus.

ICRP = International Commission on Radiological Protection; MOFSET = metal-oxide semiconductor field-effect transistor.

intended for patients with higher heart rates, the simulated heart rate was increased to 80 beats/min.

Dosimetry measurements were performed separately for the female and male phantoms. For each protocol, MOSFET readings were recorded for multiple scans, equally divided between male and female phantoms, with the phantom in the identical position for each repetition. The number of scans performed was determined according to the approach described by Trattner et al. (20) to ensure that the ED estimate was within ±10% of its true value with >90% confidence. The number of scans ranged from 4 to 10; for most protocols (84 of 120; 70%), 10 scans were performed. Scan numbers as well as additional details for each protocol are found in Online Table 1.

ED AND CONVERSION COEFFICIENT CALCULATION. We determined ED for each combination of scanner, scan mode, and voltage according to ICRP Publication 103 definition (10) as:

$$ED = \sum_{T} w_{tissue} \frac{D^{M}_{tissue} + D^{F}_{tissue}}{2}$$

where D^{M}_{tissue} and D^{F}_{tissue} are the average absorbed doses determined for each organ or tissue, *T*, for male and female phantoms, respectively. These averages were obtained over the repeated scans for each protocol. We also determined ED according to the superseded ICRP Publication 60 definition (13), which included fewer organs and some differences in tissue weightings.

Actual DLP values, as reported on the scanner console, were recorded after each scan performed. For each combination of scanner and protocol, all DLPs of repeated scans for both female and male were averaged. Each *k*-factor was determined as the ratio of the ED to the averaged DLP.

RESULTS

Cardiac *k*-factors of 12 scanners and 120 cardiac protocols (each protocol incorporating a scan mode, tube potential, and other parameter selections), calculated using the up-to-date (10) definition of ED, are presented in **Table 4**. A detailed description of each

TABLE 3 Scanners Used for Deriving *k*-Factors

Manufacturer	Scanner Model	Detector Rows for Cardiac Scanning	Source	Location
GE	LightSpeed VCT XTe	64	Single	New York-Presbyterian Hospital
GE	Discovery CT750 HD	64	Single	New York-Presbyterian Hospital
Hitachi	Scenaria	64	Single	Ocean Radiology, New York
Philips	Brilliance 64	64	Single	SUNY Downstate Medical Center, New York
Philips	Brilliance iCT 256	128	Single	Cleveland Clinic, Cleveland
Siemens	SOMATOM Sensation 64	32	Single	Cleveland Clinic, Cleveland
Siemens	SOMATOM Definition AS+	64	Single	Cleveland Clinic, Cleveland
Siemens	SOMATOM Definition	2×32	Dual	Cleveland Clinic, Cleveland
Siemens	SOMATOM Definition Flash	2×64	Dual	Cleveland Clinic, Cleveland
Siemens	SOMATOM Force*	2×96	Dual	NYU Langone Medical Center, New York
Toshiba	Aquilion 64	64	Single	New York Radiology Partners, New York
Toshiba	Aquilion Prime	80	Single	Carnegie Hill Radiology, New York
Toshiba	Aquilion ONE	320	Single	New York-Presbyterian Hospital

Tables lists scanners used in this study, including details of the manufacturer, model, and number of detector rows of each scanner and the location where dosimetry experiments took place for deriving the *k*-factors. *Used only for 70-kVp protocols (Online Table 1).

protocol is available in Online Table 1, as are additional protocols and *k*-factors at 70, 135, and 140 kVp tube potential. *k*-Factor mean and median were 0.026 $mSv \cdot mGy^{-1}cm^{-1}$, ranging between 0.020 and 0.035 $mSv \cdot mGy^{-1}cm^{-1}$ (95% confidence interval: 0.0258 to 0.0266 $mSv \cdot mGy^{-1}cm^{-1}$; coefficient of variation: 8.9%). Thus, using the European chest *k*-factor guideline of 0.014 $mSv \cdot mGy^{-1}cm^{-1}$ underestimates ED by 46%, in comparison with using an average cardiac *k*-factor, and by 30 to 60%, in comparison to using a scanner- and protocol-specific cardiac *k*-factor.

The average *k*-factor for prospectively ECG-triggered axial coronary CTA protocols was 0.0272 $mSv \cdot mGy^{-1}cm^{-1}$, slightly higher than the average *k*-factor of retrospectively ECG-gated helical coronary CTA protocols of 0.0252 $mSv \cdot mGy^{-1}cm^{-1}$. Calcium scoring scans had an average *k*-factor of 0.0289 $mSv \cdot mGy^{-1}cm^{-1}$, higher than that for coronary CTAs which averaged 0.0260 $mSv \cdot mGy^{-1}cm^{-1}$. Coronary CTA 80 kVp protocols averaged 0.0250 $mSv \cdot mGy^{-1}cm^{-1}$, lower than 100 to 120 kVp protocols, which averaged 0.0264 $mSv \cdot mGy^{-1}cm^{-1}$. Average *k*-factors for scanner models varied between 0.0229 and 0.0277 $mSv \cdot mGy^{-1}cm^{-1}$, a range of 20%. As seen in Online Table 1, 72% of the *k*-factors determined had 5% precision at a 95% confidence level, whereas 98% had 10% precision at this level. At a 90% confidence level, 80% of *k*-factors had 5% precision, and all had 10% precision.

k-Factors based on the older ICRP 60 definition of ED (13) are shown in Online Table 2, with an average *k*-factor of 0.021 $mSv \cdot mGy^{-1}cm^{-1}$. Thus, even when the same superseded definition of ED is used, calculation of ED with the chest *k*-factor of 0.014 $mSv \cdot mGy^{-1}cm^{-1}$ underestimates ED by 33% in comparison to using the average cardiac *k*-factor.

DISCUSSION

The proposed cardiac *k*-factors determined for 12 contemporary scanners and more than 120 contemporary cardiac CT protocols using the current definition of ED are all greater than the chest *k*-factor that is widely used to estimate ED from cardiac scans and is incorporated into professional society guidelines (14,15). Use of this chest *k*-factor to estimate ED results in an underestimation of ED by 46% compared with the average cardiac *k*-factor we determined and by 30 to 60%, depending on the specific scanner and protocol.

Our findings are consistent with recent findings from several other studies, each investigating a limited number of protocols (**Table 1**). All studies, including one (21) led by a member of the European Commission group which introduced the chest *k*-factor of 0.014 $mSv \cdot mGy^{-1} \cdot cm^{-1}$, found considerably higher *k*-factors, also varying among scanners and protocols and ranging from 0.020 to 0.043 $mSv \cdot mGy^{-1} \cdot cm^{-1}$. Given our findings, together with this supportive data, we believe that the use of the European Commission chest *k*-factor to estimate ED in cardiac CT, a practice never endorsed by the European Commission or American Association of Physicists in Medicine, should be reconsidered. For a better estimation of ED, we propose that, ideally, a scanner- and protocol-specific factor be used, and if one is not easily available, then we recommend use of our mean (as well as median) *k*-factor of 0.026 $mSv \cdot mGy^{-1} \cdot cm^{-1}$.

Several factors contribute to this difference between cardiac and chest *k*-factors. One factor is a fundamental distinction between cardiac scans, which typically involve approximately 12 to 14 cm of craniocaudal coverage, and thoracic scans covering the entire chest, which spans approximately 27 cm craniocaudally. Although all or most of the breast tissue is typically irradiated in both cardiac and chest CT scans, chest scans extend both cranially and caudally to include areas without breast tissue, and thus, there is more breast irradiation per length scanned in cardiac CT. Because the breasts are highly radiosensitive organs, one should expect a higher *k*-factor for a cardiac scan (22,23). Additionally, most vendors of CT scanners used in this study report using different "bow tie" filters for cardiac and chest scans, which is another factor which contributes to the difference between cardiac and chest *k*-factors.

Another contributor to the difference between our cardiac *k*-factors and the European chest scan *k*-factor is the definition of ED used. The older definition resulted, for cardiac scans, in a *k*-factor that is 21% lower than that in the current ED definition. The primary driver of this difference is the updated tissue weighting factors determining each organ's contribution to the whole-body ED, which are incorporated in ICRP 103 ED definition to better reflect the current state of radiation epidemiological data. In particular, the tissue weighting factor for the breast increased from 0.05 to 0.12. Because the breast is directly irradiated by the x-ray beam in cardiac scans, it has a high organ radiation dose and, together with lung dose, is the main organ contributing to the ED from cardiac CT. Additionally, in the ICRP 103 formulation of ED, the heart is included among the "remainder organs," whereas previously the heart had not been assigned a tissue weighting factor and thus did not contribute to ED. The update in the tissue weighting factors, which is not reflected in the European Commission chest *k*-factor, is another source for ED underestimation using this factor.

An additional limitation of the European guidelines chest conversion factor of 0.014 $mSv \cdot mGy^{-1} \cdot cm^{-1}$

TABLE 4 Conversion Factors Relating Effective Dose to Dose-Length Product, Using Current Definition of Effective Dose

ICRP 103	Prospective Axial			Prospective Axial Padding			Prospective Helical		
Scanner/kVp	80	100	120	80	100	120	80	100	120
GE Lightspeed VCT XTe	0.0259	0.0298	0.0295	0.0263	0.0283	0.0290	x	x	x
GE Discovery CT750 HD	x	0.0302	x	0.0262‡	0.0278‡	0.0283‡	x	x	x
Hitachi Scenaria	0.0254	0.0272	0.0277	0.0260	0.0268	0.0281	x	x	x
Philips Brilliance 64	x	x	x	x	x	x	x	x	x
Philips Brilliance iCT 256	0.0301	0.0314	0.0316	0.0279	0.0295	0.0303	x	x	x
Siemens SOMATOM Sensation 64	0.0264	0.0268	0.0266	x	x	x	x	x	x
Siemens SOMATOM Definition AS+	0.0271	0.0275	0.0273	0.0256	x	0.0257	x	x	x
Siemens SOMATOM Definition	0.0288	0.0288	0.0274	x	x	x	x	x	x
Siemens SOMATOM Definition FLASH	0.0253	0.0266	0.0254	0.0240	0.0252	0.0256	0.0263	0.0268	0.0266
Toshiba Aquilion 64	x	x	x	x	x	x	x	x	x
Toshiba Aquilion Prime	x	x	x	x	x	x	0.0209	0.0229	0.0242
Toshiba Aquilion ONE	x	0.0227‖	0.0250‖	0.0229¶	0.0259¶	0.0261¶	x	x	x
Average, per protocol type & kV	0.0270	0.0279	0.0276	0.0256	0.0273	0.0277	0.0236	0.0248	0.0254
CV, %	6.8	9.2	7.8	6.1	5.4	6.2	16.0	10.9	6.6
Average, per protocol type, all kV		0.0275			0.0269			0.0246	
CV, %		7.9			6.6			9.6	
Average, all prospective axial (with and without padding)			0.0272						
CV, %			7.3						
Average, all protocols (prospective, retrospective, and calcium scoring)					0.0262				
CV, %					8.9				

TABLE 4 Continued

ICRP 103	Retrospective Helical			Retrospective Helical TCM*			Calcium		
Scanner/kVp	80	100	120	80	100	120	120	Average	CV [%]
GE Lightspeed VCT XTe	0.0242	0.0267	0.0264	0.0243	0.0259	0.0269	0.0306†	0.0275	8.0
GE Discovery CT750 HD	x	0.0284	0.0267	x	0.0268	0.0269	0.0285	0.0277	4.4
Hitachi Scenaria	0.0258	0.0272	0.0281	x	x	x	0.0265	0.0269	3.5
Philips Brilliance 64	0.0249	0.0260	0.0261	0.0246	0.0260	0.0267	0.0285	0.0261	4.9
Philips Brilliance iCT 256	0.0242§	0.0254§	0.0254§	0.0231	0.0248	0.0249	x	0.0274	11.2
Siemens SOMATOM Sensation 64	0.0250	0.0249	0.0249	0.0256	0.0253	0.0251	x	0.0256	3.0
Siemens SOMATOM Definition AS+	0.0243	0.0251	0.0246	0.0244	0.0252	0.0250	x	0.0256	4.6
Siemens SOMATOM Definition	0.0259	0.0286	0.0262	0.0271	0.0287	0.0281	x	0.0277	4.1
Siemens SOMATOM Definition FLASH	0.0203	0.0256	0.0256	0.0230	0.0243	0.0248	x	0.0250	6.7
Toshiba Aquilion 64	x	0.0241	0.0252	x	0.0231	0.0236	0.0349	0.0262	18.8
Toshiba Aquilion Prime	0.0208	0.0231	0.0232	0.0212	0.0233	0.0234	0.0256	0.0229	6.7
Toshiba Aquilion ONE	x	x	x	x	x	x	0.0257	0.0247	6.2
Average, per protocol type & kV	0.0239	0.0259	0.0257	0.0242	0.0253	0.0256	0.0289		
CV, %	8.6	6.6	4.9	7.3	6.6	6.0	10.9		
Average, per protocol type, all kV		0.0253			0.0251				
CV, %		7.3			6.8				
Average, all retrospective helical (with and without TCM)			0.0252						
CV, %			7.0						
Average, all protocols (prospective, retrospective, and calcium scoring)					0.0262				
CV, %					8.9				

Scanner- and protocol-specific *k*-factors, in units of $mSv \cdot mGy^{-1}cm^{-1}$, were calculated for cardiac CT using ICRP Publication 103 definition of effective dose, for 12 scanners and 120 scan protocols with standard tube potentials of 80, 100, and 120 kVp. *k*-Factors here are summarized in 5 categories of axial and helical CT angiography protocol types, and calcium score. Per-scanner averages of the *k*-factors across all protocol types and energy levels are displayed along with the CV in the 2 right-most columns. Scan length for all scans is 13.3 to 14.2 cm. Heart rate is 60 beats/min for all scans, except where otherwise noted. A detailed description of each protocol here is also provided in Online Table 1, as are additional *k*-factors and detailed descriptions for very low (70 kVp) and high (135 or 140 kVp) tube potential protocols for selected scanners. *Tube current modulation. †Average of 2 beams with 20- and 40-mm widths. ‡Heart rate = 80 beats/min (all others are 60 beats/min). §Average of high and standard resolution modes. ‖Target mode volume scan. ¶Continuous volume scan with exposure throughout a full cardiac cycle.

CV = coefficient of variation (ratio of standard deviation to mean in percentage values); other abbreviations as in Tables 1 to 3.

is that it was determined based on modeling 3 now-antiquated single-slice scanners, none of which were capable of performing coronary CTA (Siemens DRH [Siemens, Munich, Germany], GE 9800 [GE, Hannover, Maryland], and Philips LX [Philips, Amsterdam, the Netherlands]). The use of these old scanners for contemporary cardiac CT dosimetry should no longer be considered applicable. Moreover, as noted above, the very same European guidelines document, in another appendix which considered some more recent scanners (up to 16-slice), already suggested a higher (noncardiac) chest conversion factor of 0.019 $mSv \cdot mGy^{-1} \cdot cm^{-1}$.

STUDY LIMITATIONS. Our study has a few potential limitations. There are several experimental and computational components to the determination of a *k*-factor, each with associated uncertainty. These components include the scanner-reported DLP, effective energy calculation, energy dependent absorption coefficients, and MOSFET measurement and calibration (16). However, we performed repeated measurements to ensure that ED determination had high precision with high confidence, using the scheme of Trattner et al. (20). Additionally, we performed most scans with a simulated heart rate of 60 beats/min without heart rate variability. Fluctuations in heart rate or higher rates that cannot be controlled have the potential to alter data acquisition and impact the *k*-factor. However, in a recent MOSFET study in pediatric cardiac CT, Trattner et al. (23) found no impact of heart rate on *k*-factor. The use of up to 44 MOSFETs simultaneously raises a question of a potential impact of the wires on the measured dose levels and hence on the *k*-factors. However, we have tested such impact using a pediatric phantom with 50 MOSFETs which were more densely placed than in the adult phantom here and found that individual *k*-factors typically varied by only $\pm 0.001\ mSv \cdot mGy^{-1} \cdot cm^{-1}$ depending on whether or not all 50 MOSFETs were placed simultaneously (23). The effective energy values used to determine the *f*-factors above refer to the energy just upon entrance to the phantom's body and not at the exact location of the MOSFET. However, experiments we performed using various protocols in one scanner demonstrated the difference in simulated effective energy in the exact MOSFET location versus simulated effective energy upon entrance to the phantom body was approximately 1%, a sufficiently low error to justify the use of body-entrance effective energy values. Finally, ED is more formally defined computationally, and our approach was largely experimental. Our motivation was to avoid the need to make assumptions regarding proprietary aspects of scanner design and protocols, which would have been required for Monte Carlo simulation. Even so, for a single scanner, we have compared MOSFET to Monte Carlo estimation of effective dose and found outstanding agreement (24).

CONCLUSIONS

We determined cardiac-specific conversion factors for contemporary scanners and routinely used clinical protocols to enable a more accurate estimation of ED, given a scanner-reported DLP, as compared to estimation utilizing the commonly used factor of 0.014 $mSv \cdot mGy^{-1} \cdot cm^{-1}$. Although mentioned in current guidelines, this latter factor was determined for chest rather than cardiac CT, based on now-obsolete single-slice scanners and using a now-outdated definition of ED. The cardiac-specific factors we determined are, for all 12 scanners and 120 scan protocols used, considerably higher than the chest conversion factor, suggesting that radiation doses from cardiac CT have been significantly and systematically underestimated. We suggest that, ideally, a scanner- and protocol-specific conversion factor should be used for estimating ED from cardiac CT, or if scanning information is unavailable, then one should use our mean and median conversion factor of 0.026 $mSv \cdot mGy^{-1} \cdot cm^{-1}$. The use of cardiac-specific factors is critical to ensure more accurate dosimetry to inform the benefit-risk calculus of cardiac imaging strategies, and optimize radiation safety of patients.

ACKNOWLEDGMENTS The authors thank Richard Maldonado, Sheldon Herbert, Ted Pozniakoff, Ketan Bhatia, Amsale Robi, Tony Zapata, Carlos DeOleo, and Jose Casado (New York-Presbyterian Hospital); Michael Manning (Cleveland Clinic), Donna McKenzie (SUNY Downstate Medical Center); Carol Murphy (NYU Langone Medical Center); and Steven Wolff (Carnegie Hill Radiology) for administrative and technical assistance in scanning. We also thank Grant Stevens (GE), Donald Bosele (Hitachi), Peter Prinsen and Tom Morton (Philips), Tom O'Donnell (Siemens), and Di Zhang and Erin Angel (Toshiba) for technical information regarding scanners, Abdelbasset Hallil (Best Medical) for information regarding and technical support for MOSFETs, and Pamela Douglas (Duke), Udo Hoffmann (MGH), and Brian Ghoshhajra (MGH) for helpful comments on the manuscript.

ADDRESS FOR CORRESPONDENCE: Dr. Andrew J. Einstein, Columbia University Medical Center, Department of Medicine, Division of Cardiology, 622 West 168th Street, PH 10-203B, New York, New York 10032. E-mail: andrew.einstein@columbia.edu.

PERSPECTIVES

COMPETENCY IN MEDICAL KNOWLEDGE: New methodology introduced here provides more accurate tools to estimate radiation effective dose from cardiac CT scans.

COMPETENCY IN PATIENT CARE AND PROCEDURAL SKILLS: Updated methodology for determining radiation dose from cardiac CT should be used to enhance the benefit-risk calculus of cardiac imaging strategies and optimize test and protocol selection.

TRANSLATIONAL OUTLOOK: The use of a more accurate methodology for estimating radiation dose from CT may affect the balance of benefits and risks of cardiac imaging strategies. Additional studies are needed, incorporating this methodology as well as updated dosimetry methodology for other modalities, to reassess the comparative effectiveness of strategies for managing patients with chest pain and other clinical scenarios requiring cardiovascular evaluation.

REFERENCES

1. Greenland P, Alpert JS, Beller GA, et al. 2010 ACCF/AHA guideline for assessment of cardiovascular risk in asymptomatic adults: a report of the American College of Cardiology Foundation/American Heart Association Task Force on Practice Guidelines. J Am Coll Cardiol 2010;56:e50–103.

2. Budoff MJ, Nakazato R, Mancini GB, et al. CT angiography for the prediction of hemodynamic significance in intermediate and severe lesions: head-to-head comparison with quantitative coronary angiography using fractional flow reserve as the reference standard. J Am Coll Cardiol Img 2016;9:559–64.

3. Hadamitzky M, Achenbach S, Al-Mallah M, et al. Optimized prognostic score for coronary computed tomographic angiography: results from the CONFIRM registry (COronary CT Angiography EvaluatioN For Clinical Outcomes: An InteRnational Multicenter Registry). J Am Coll Cardiol 2013;62:468–76.

4. Goldstein JA, Chinnaiyan KM, Abidov A, et al. The CT-STAT (Coronary Computed Tomographic Angiography for Systematic Triage of Acute Chest Pain Patients to Treatment) trial. J Am Coll Cardiol 2011;58:1414–22.

5. Douglas PS, Hoffmann U, Patel MR, et al. Outcomes of anatomical versus functional testing for coronary artery disease. N Engl J Med 2015;372:1291–300.

6. CT coronary angiography in patients with suspected angina due to coronary heart disease (SCOT-HEART): an open-label, parallel-group, multicentre trial. Lancet 2015;385:2383–91.

7. Einstein AJ, Henzlova MJ, Rajagopalan S. Estimating risk of cancer associated with radiation exposure from 64-slice computed tomography coronary angiography. JAMA 2007;298:317–23.

8. Schuhbaeck A, Achenbach S, Layritz C, et al. Image quality of ultra-low radiation exposure coronary CT angiography with an effective dose <0.1 mSv using high-pitch spiral acquisition and raw data-based iterative reconstruction. Eur Radiol 2013;23:597–606.

9. Lu MT, Douglas PS, Udelson JE, et al. Safety of coronary CT angiography and functional testing for stable chest pain: a randomized comparison of test complications, incidental findings and radiation dose. Submitted 2017.

10. International Commission on Radiological Protection. ICRP Publication 103. The 2007 recommendations of the International Commission on Radiological Protection. Ann ICRP 2007;37:1–332.

11. Martin CJ. Effective dose: how should it be applied to medical exposures? Br J Radiol 2007;80:639–47.

12. McCollough CH, Christner JA, Kofler JM. How effective is effective dose as a predictor of radiation risk? AJR Am J Roentgenol 2010;194:890–6.

13. International Commission on Radiological Protection. ICRP publication 60. The 1990 recommendations of the International Commission on Radiological Protection. Ann ICRP 1991;21:1–201.

14. Bongartz G, Golding SJ, Jurik AG, et al. European guidelines for multislice computed tomography. Luxembourg: European Commission, 2004.

15. American Association of Physicists in Medicine. The measurement, reporting, and management of radiation dose in CT. Report no. 96. College Park, MD: American Association of Physicists in Medicine, 2008.

16. Trattner S, Prinsen P, Wiegert J, et al. Calibration and error analysis of metal-oxide-semiconductor field-effect transistor dosimeters for computed tomography radiation dosimetry. Med Phys, conditionally accepted 2017.

17. Bushberg JT, Seibert JA, Leidholdt EM, Boone JM. The Essential Physics of Medical Imaging. 3rd edition. Philadelphia: Lippincott Williams & Wilkins; 2012.

18. Eckerman KF, Bolch WE, Zankl M, Petoussi-Henss N. Response functions for computing absorbed dose to skeletal tissues from photon irradiation. Radiat Prot Dosimetry 2007;127:187–91.

19. Einstein AJ, Elliston CD, Arai AE, et al. Radiation dose from single-heartbeat coronary CT angiography performed with a 320-detector row volume scanner. Radiology 2010;254:698–706.

20. Trattner S, Cheng B, Pieniazek RL, Hoffmann U, Douglas PS, Einstein AJ. Sample size requirements for estimating effective dose from computed tomography using solid-state metal-oxide-semiconductor field-effect transistor dosimetry. Med Phys 2014;41:042102.

21. Geleijns J, Joemai RM, Dewey M, et al. Radiation exposure to patients in a multicenter coronary angiography trial (CORE 64). AJR Am J Roentgenol 2011;196:1126–32.

22. Huda W, Tipnis S, Sterzik A, Schoepf UJ. Computing effective dose in cardiac CT. Phys Med Biol 2010;55:3675–84.

23. Trattner S, Chelliah A, Ruzal-Shapiro CB, et al. Estimating effective dose of radiation from pediatric cardiac CT angiography using a 64-slice scanner: new conversion factors relating dose-length product to effective dose. AJR Am J Roentgenol 2017;208:585–94.

24. Prinsen P, Wiegert J, Trattner S, et al. High correlation between CT radiation dose estimates obtained by fast monte carlo computation and solid-state metal-oxide semiconductor field-effect transistor measurements in physical anthropomorphic phantoms. European Congress of Radiology Abstracts 2014:B-0245.

25. Gosling O, Loader R, Venables P, Rowles N, Morgan-Hughes G, Roobottom C. Cardiac CT: are we underestimating the dose? A radiation dose study utilizing the 2007 ICRP tissue weighting factors and a cardiac specific scan volume. Clin Radiol 2010;65:1013–7.

26. Gosling OE, Roobottom CA. Radiation exposure from cardiac computed tomography. J Am Coll Cardiol Img 2010;3:1201–2.

27. Fink C, Krissak R, Henzler T, et al. Radiation dose at coronary CT angiography: second-generation dual-source CT versus single-source 64-MDCT and first-generation dual-source CT. AJR Am J Roentgenol 2011; 196:W550–7.

28. Christner JA, Kofler JM, McCollough CH. Estimating effective dose for CT using dose-length product compared with using organ doses: consequences of adopting International Commission on Radiological Protection publication 103 or dual-energy scanning. AJR Am J Roentgenol 2010; 194:881–9.

29. Goetti R, Leschka S, Boschung M, et al. Radiation doses from phantom measurements at high-pitch dual-source computed tomography coronary angiography. Eur J Radiol 2012;81: 773–9.

30. Seguchi S, Aoyama T, Koyama S, Fujii K, Yamauchi-Kawaura C. Patient radiation dose in prospectively gated axial CT coronary angiography and retrospectively gated helical technique with a 320-detector row CT scanner. Med Phys 2010;37: 5579–85.

KEY WORDS cardiac computed tomography, conversion factors, radiation dose

APPENDIX For an expanded Methods section as well as supplemental figures and tables, please see the online version of this article.